Research article

Studying social awareness of physical distancing in mitigating COVID-19 transmission

Xiaoying Wang*

Department of Mathematics, Trent University, Peterborough, ON K9L 0G2, Canada

* **Correspondence:** Email: xiaoyingwang@trentu.ca; Tel: +17057481011 x7614.

Abstract: Since the initial identification of a COVID-19 case in Wuhan, China, the novel disease quickly becomes a global pandemic emergency. In this paper, we propose a dynamic model that incorporates individuals' behavior change in social interactions at different stages of the epidemics. We fit our model to the data in Ontario, Canada and calculate the effective reproduction number $\mathcal{R}_t$ within each stage. Results show that $\mathcal{R}_t > 1$ if the public's awareness to practice physical distancing is relatively low and $\mathcal{R}_t < 1$ otherwise. Simulations show that a reduced contact rate between the susceptible and asymptomatic/unreported symptomatic individuals is effective in mitigating the disease spread. Moreover, sensitivity analysis indicates that an increasing contact rate may lead to a second wave of disease outbreak. We also investigate the effectiveness of disease intervention strategies. Simulations demonstrate that enlarging the testing capacity and motivating infected individuals to test for an early diagnosis may facilitate mitigating the disease spread in a relatively short time. Results also indicate a significantly faster decline of confirmed positive cases if individuals practice strict physical distancing even if restricted measures are lifted.

Keywords: COVID-19; piecewise model; social awareness; disease mitigation strategy; epidemic model

1. Introduction

The coronavirus disease 2019 (COVID-19) has become a public heath emergency worldwide and has brought unprecedented challenges to the entire society. This novel disease was initially identified in Wuhan, which is a city with a dense population in China. Since its initial discovery in late December 2019, the disease soon spread worldwide and caused over $17,106,000$ total infections and more than $668,900$ deaths until July 30, 2020 [1].

Similar to other coronaviruses, this novel pneumonia is transmitted primarily via close contact between susceptible and infected individuals [1]. Studies also show that the virus can survive on object

surfaces from a few hours to a few days, which leads to possible disease transmission through touching contaminated surfaces [2]. Also, the disease is highly transmissible, not only from symptomatic infected individuals to susceptible population, but also from asymptomatic carriers to susceptible individuals [3–6]. Currently, there are no vaccines available and therefore the main intervention strategies of disease transmission are nonpharmaceutical. The aforementioned characteristics of the disease transmission impose difficulties to mitigate the disease outbreak.

The first confirmed positive case of COVID-19 in Ontario, Canada was identified on January 28, as a person who had traveled to Wuhan during that time [7]. The number of confirmed infected population in Ontario remained low in February (less than 10 in total) and all the positive cases were travel related. However, the disease transmission escalated rapidly starting early March. Evidence of community transmission was identified and the first deceased case with no travel history or close contact in Ontario was recorded on March 17 [7]. Soon after that, Ontario became one of the provinces in Canada with the most severe disease infection.

The rapidly deteriorated disease status raised serious concerns among public heath specialists and in public. As a result, the Ontario government declared a state of emergency and ordered the closure of all nonessential businesses on March 17. Restrictive measures are effective in mitigating the disease spread in a short-term but also lead to huge economic loss and social disruption. As a vital part of the nonpharmaceutical intervention, people were instructed to keep a physical distancing when appeared in public. This measure is expected to reduce the probability of infection for an individual because it reduces the contact rate between the susceptible and infected individuals. However, the effectiveness of this measure depends largely on the awareness and cooperation of the public and how individuals practice physical distancing in daily social activities.

Starting in May, with a steady decline of the daily confirmed cases, a number of nonessential businesses reopened according to Ontario government's multi-phase reopening plan. The lift of stringent measures is associated with risks of a second wave of the disease spread. More importantly, the reopening may serve as a message indicating less severity of the disease and inevitably changes individuals' behavior. This further leads to an increasing probability of infection if individuals do not practice physical distancing effectively.

Since the initial disease outbreak, mathematical models have been used widely to predict the trend of disease spread and study the mitigation strategies (see [8–16] for example). Both deterministic and stochastic models are fitted to data in different geographical regions, including Ontario Canada, see [17–20] for example. However, many of the fittings are based on data at early stages of the disease outbreak only. While the aforementioned results are valuable, models calibrated for early stages do not incorporate individuals' behavior change induced by social awareness.

In this paper, we propose a dynamic model where the contact rate between susceptible and infected individuals varies with the different severity of disease spread. The model is fitted to the data in Ontario, Canada for illustration. The main objective of this paper is to study the role of social awareness in practicing physical distancing in mitigating the disease spread. We also make short-term predictions about the disease outbreak, assuming that businesses reopen and the practice of physical distancing is loosened.

2. Methods

2.1. Data

The COVID-19 data in Ontario is publicly accessible and contains information such as reporting date, daily number of confirmed cases, daily completed tests, current number of patients who are in intensive care units (ICU) etc. The data is collected from 34 heath units across Ontario and is updated on a daily basis [7]. As discussed above in the Introduction, both the number of cumulative infected cases and the number of reported symptomatic cases remained quite low in January and February and hence are not included in the figures below.

Figure 1(a) shows the number of cumulative confirmed cases of COVID-19 from March 2 to May 18. It clearly indicates an exponential growth of the confirmed cases in an early stage of the disease spread. Figure 1(b) shows the daily number of positive cases who are still actively contagious. The data in Figure 1(b) excludes the disease related deaths and the recovered individuals. In Ontario, instructed by the Ministry of Heath, recovered cases are defined as confirmed infected individuals who are hospitalized but recover from the disease or individuals who are not hospitalized but are over a 14-days period since the reporting date of infection [7].
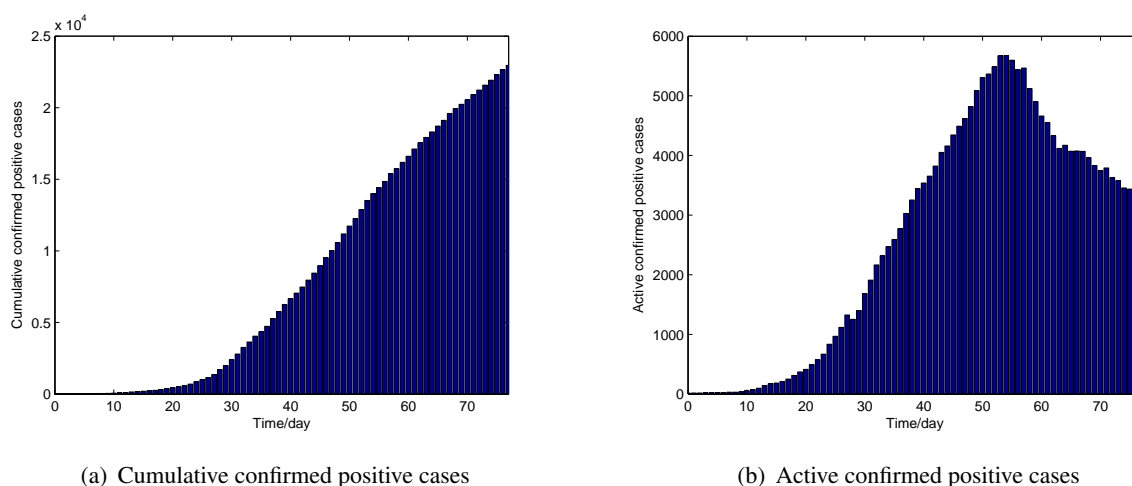

(a) Cumulative confirmed positive cases   (b) Active confirmed positive cases

Figure 1. Panel 1(a) and panel 1(b) show data from March 2 to May 18, 2020, in Ontario, Canada. 1(a) demonstrates the cumulative confirmed cases; 1(b) indicates the daily confirmed cases who are still active in transmitting the disease.

2.2. The model

We propose a compartmental model based on different status of individuals in the epidemics, as shown in diagram 2. The model is stratified to include the following classes: susceptible (S), exposed (E), asymptomatic (A), symptomatic but not reported to public heath agencies (U), symptomatic and isolated or hospitalized (I), and recovered (R).

In this model, we assume that individuals in the exposed class (E) as individuals who have contracted the COVID-19 virus but are in the incubation period and are not contagious yet. Asymptomatic individuals (in the compartment A) are individuals who are infected with the virus but do not show
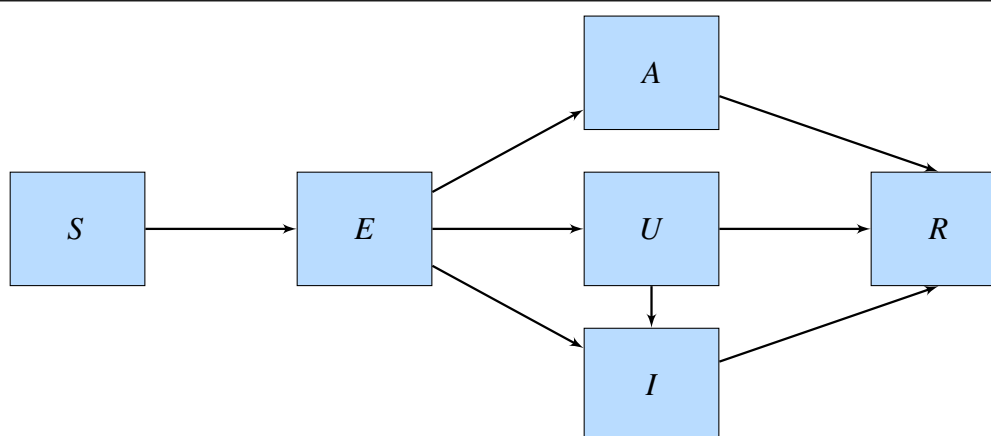
Figure 2. The flow chart for model (2.3).

symptoms of infection. Unreported infected class (U) includes individuals who have contracted the virus but merely show mild symptoms and therefore do not visit medical facilities for diagnosis. Individuals who show symptoms of infection and report themselves to public heath agencies are classified as the reported infected class (I).

We assume that only asymptomatic and unreported infected individuals (in compartments A, U) are contagious and may transmit the disease. In compliance with the disease intervention policies in Ontario, reported infected individuals are either self-isolated at home assuming they experience mild to moderate symptoms or hospitalized if they develop serious symptoms. In either way, the confirmed cases are monitored and actively isolated from the susceptible community and hence have very low risk of transmitting the disease. Infected individuals may move to the recovered class (R) if they are cured of the disease and are no longer contagious.

Susceptible individuals may contract the virus via contacting the infected individuals and move to the exposed class. During the pandemic, disease intervention strategies such as closure of all nonessential businesses reduce the contact rate between susceptible and infected individuals to a large extent but certainly cannot disrupt all social activities. The effectiveness of these measures still depends largely on how individuals practice physical distancing. Individuals are prone to reduce social activities and take extra precautious measures to prevent infection if they consider the disease spread as severe. However, on the other side, individuals may relax the practicing of physical distancing if they evaluate the risk of being infected as low.

During the pandemic, individuals have easy access to media reporting, where daily confirmed number of infected population is updated and broadcasted in a timely manner. Naturally, the reported infected population serves as a direct indicator about the severity of disease. This together with government policies inevitably alter individual behaviors and affect the effectiveness of practicing physical distancing.

Therefore, it is more important to assume that the contact rate between susceptible and infected individuals changes at different stages of the epidemics, rather than a constant at all time. We assume the contact rate as

$$\beta_1(1 - f(I)), \tag{2.1}$$

where β_1 is the baseline contact rate in a disease-free status and $f(I)$ represents the contact rate reduc-

tion due to the practice of physical distancing. To start with the simplest model, we propose $f(I)$ to be a piecewise function as

$$f(I) = \begin{cases} \alpha_1, & \text{if} \quad 0 < I < I_1, \\ \alpha_2, & \text{if} \quad I_1 < I < I_2, \\ \alpha_3, & \text{if} \quad I_2 < I, \end{cases} \tag{2.2}$$

where α_i are constants with the relation $\alpha_1 < \alpha_2 < \alpha_3 < 1$, and I_1, I_2 are constants with $I_1 < I_2$. The piecewise contact rate (2.2) reflects the progression of the extent and effectiveness of disease intervention strategies when the disease enters different stages. The contact rate is reduced to a larger extent if the reported infected population is larger. However, the contact rate cannot be reduced infinitely and must attain a minimum value of $\beta_1(1 - \alpha_3)$ because essential social activities are inevitable. It is worthwhile to mention that in [15], the authors also studied the effectiveness of media reporting in reducing the COVID-19 spread but they proposed a different model by incorporating the media number as a state variable. Here, we model the media impact implicitly but associate its impact with an individual's behavior change that reflects on the contact rate reduction on the community level.

Based on the aforementioned discussions, we propose the dynamic model as

$$\begin{aligned} \frac{dS}{dt} &= -\beta_1(1 - f(I))AS - \beta_2(1 - f(I))US \\ \frac{dE}{dt} &= \beta_1(1 - f(I))AS + \beta_2(1 - f(I))US - \mu E \\ \frac{dA}{dt} &= \mu \rho_1 E - \eta_1 A \\ \frac{dI}{dt} &= \mu(1 - \rho_1 - \rho_2)E + \tau U - \eta_3 I - \delta I \\ \frac{dU}{dt} &= \mu \rho_2 E - \eta_2 U - \tau U \\ \frac{dR}{dt} &= \eta_1 A + \eta_2 U + \eta_3 I, \end{aligned} \tag{2.3}$$

where $f(I)$ is defined above in (2.2) and the other parameters are summarized in Table 1 in Section 3.

2.3. The reproduction number

The effective reproduction number $\mathcal{R}_t$ is defined as the average secondary infections caused by an infected individual at a time event t. By its definition, it serves as a threshold to predict the disease spread. The disease spread increases at time t if the effective reproduction number is larger than 1 but declines if the reproduction number is smaller than 1. The effective reproduction number extends the basic reproduction number $\mathcal{R}_0$ and reflects the decline of susceptible population. Let S_t denote the susceptible population at time t. In [21, 22], the authors showed that for an autonomous model where parameters are constants, the effective reproduction number satisfies $\mathcal{R}_t = (S_t/S_0)\mathcal{R}_0$. We calculate the basic reproduction number $\mathcal{R}_0$ of (2.3) by using the next generation matrix method for compartmental models [23].

Direct calculations lead to the effective reproduction number as

$$\mathcal{R}_t = \frac{(1 - f(I_t)) \left[\beta_1 \rho_1 \eta_2 + \beta_1 \rho_1 \tau + \beta_2 \eta_1 \rho_2 \right] S_t}{\eta_1 (\eta_2 + \tau)}, \tag{2.4}$$

where $f(I_t)$ is defined in (2.2). Because the contact rate reduction term $f(I_t)$ is defined as a piecewise function, we expect to obtain different $\mathcal{R}_t$ in each interval of I. We will estimate the values of I_1, I_2 that best fit the data and calculate $\mathcal{R}_t$ accordingly in the following analysis.

2.4. Parameter estimation

In (2.3), ρ_1 represents the proportion of exposed individuals who eventually move to the asymptomatic class, ρ_2 is the proportion that goes to the unreported infected class, and the remaining $(1 - \rho_1 - \rho_2)$ proportion moves to the reported infected class. We find reasonable ranges for ρ_1 and ρ_2 from [24–26]. Mizumoto et al. analyzed the data that documented the passengers on the *Diamond Princess* cruise ship and found that 18% of the passengers never developed symptoms [24]. Nishiura et al. studied evacuees from Wuhan to Japan and found that 31% of the evacuees who tested positive infection of COVID-19 virus never showed any symptoms [25]. Considering that the majority of passengers from the *Diamond Princess* cruise ship are at older ages, who are more likely to develop symptoms once being infected, it is safe to assume that $\rho_1 = 30\%$. A recent statistical based study of the COVID-19 outbreak in Wuhan [26] showed that 59% of the individuals exposed to the virus did not show symptoms or only showed mild symptoms and therefore were not recorded by the public heath agency. Overall, among a homogeneous population, it is reasonable to believe that asymptomatic and unreported infected individuals with mild symptoms consist of 50–60% of the total infected population. Equivalently, in model (2.3), this evidence suggests that $\rho_1 + \rho_2 = 50$–60%, which leads to $\rho_2 = 20$–30%. In our simulation, we fix $\rho_2 = 30\%$ to fit the data.

In [5], the authors showed that the average incubation period for an individual from being exposed to the COVID-19 virus to the symptom onset is 5.2 days. In a separate study [3], the authors showed that a person exposed to the virus may shed the virus and be contagious 48 to 72 hours before starting to experience symptoms. In (2.3), individuals in the exposed class (E) are infected with the virus but are not yet contagious. Hence, it is reasonable to assume that the transition rate from exposed class to asymptomatic class/unreported infected class/reported infected class as $\mu = 1/3$.

Due to the course of infection, a patient may experience a sudden deteriorated heath condition and seek for medical help at a later stage [27]. As a consequence, individuals from the unreported infected class with mild symptoms may move to the reported infected class at a rate of τ. The parameter τ is estimated from data fitting via the MCMC algorithm.

In (2.3), asymptomatic individuals, unreported infected individuals and reported infected individuals progress to the recovered compartment at a rate of η_1, η_2, η_3 respectively. In [10], the authors studied the importance of detecting the unreported infected cases in controlling the COVID-19 in Wuhan, China. The authors assumed that the recovery rate of infected individuals that include both reported and unreported classes varied between 1/7–1 and found that 1/7 provided the best fitting. Hence, in our model, it is reasonable to assume that $\eta_1 = \eta_2 = 1/7 = \eta_3 = 1/7$.

The total number of residents in Ontario is 14570000, which gives $S_0 = 14570000$. The number of active infected cases at initial time (April 16 from the data) is 4344 and therefore $I_0 = 4344$. The initial population of exposed class (E_0), asymptomatic class (A_0), and unreported infected class (U_0) are estimated from the MCMC simulations respectively.

The baseline contact rates between susceptible and asymptomatic/unreported symptomatic individuals β_1, β_2 are set to be identical because there is no significant social interaction difference between these groups.

We fit our model to data by the Markov Chain Monte Carlo (MCMC) method and adopt the adaptive Metropolis-Hastings algorithm to carry out this approach [28]. The algorithm is run for 10,000 iterations with a burn-in of the first 7000 iterations. Geweke convergence test is employed to diagnose the convergence of the Markov chains.

The estimated parameters and initial data are listed in Table 1. The model (2.3) is fitted to the data from April 16 to May 18 in particular. Figure 1 shows that the reported infected population undergoes two different stages of growth. Both Figures 1(a), 1(b) indicate that the reported infected population grows exponentially in the entire March and in early April. Followed by that, the growth rate slows down but the daily reported infected population continues to increase until late April. There are a number of reasons why the reported infected population increases in two distinct stages. One reason is that in the early stage, the disease outbreak risk in Canada was believed to be low and as a result, social activities among public remained unchanged. Starting mid March, aggressive measures such as school closure, shutting down of all non-essential businesses, mandatory 14-days self-isolation for all travelers etc. have been imposed by the government. Consequently, the contact rate between susceptible population and infected population has been reduced by a large extent.

Another important reason for the two-stage growth is the significant increase in testing capacity over time. In Ontario, the daily number of testing starts as low as 2000 provincial wide in the early stage and ramps up to as high as 20000 later, which is the province's target. Unfortunately, the data set in [7] doesn't include records of the daily testing number for the dates before April 15. To avoid large noise in data caused by the testing capacity, the model is fitted to a period where the daily testing finished remains relatively stable, i.e., between April 16 and May 18. After that, Ontario moves into the first stage of reopening and a testing policy targeting at wider communities has been updated, which inevitably affects the social interaction patterns and testings.

3. Results

(1) Fitting results

By fitting model (2.3) to the data in Figure 1(b) via the MCMC algorithm, we obtain the result, as indicated in Figure 3. Figure 3(a) shows a good fit of the model solution $I(t)$ and the data of reported infected population. Figure 3(b) demonstrates the predictive envelopes of the 95% credible interval. The fitting indicates that under the current social distancing measures, the number of active infected cases will decline steadily over a period of approximately 140 days until reaches a flattened plateau phase. The total number of reported infected population will decline to approximately 950, within a range of $500 - 1500$. The prediction indicates that the disease will not likely die out in a short amount of time but rather persist in communities over a relatively long period. However, if we compare the peak value of reported symptomatic population with the predictive number of reported symptomatic cases who will enter the plateau phase, we find a significant decline. Although active symptomatic cases will not drop drastically to 0, controlling this number at a relatively low level could alleviate the stress of the entire heath care system. This suggests that current disease intervention strategies combined with adequate awareness from the public of practicing the physical distancing are effective in preventing a further outbreak.

Next we analyze further why the disease intervention strategies and social awareness are effective in mitigating the disease spread. As calculated in (2.4), the effective reproduction number serves as

Table 1. Parameter estimates for the COVID-19 epidemics in Ontario, Canada.

Parameter	Definition	Estimated Mean Value	Standard Deviation	Data Source
β_1	Contact rate between S and A	5.3533×10^{-8}	3.4044×10^{-9}	MCMC
β_2	Contact rate between S and U	5.3533×10^{-8}	3.4044×10^{-9}	MCMC
α_1	Contact rate reduction 1	0.1288	0.011	MCMC
α_2	Contact rate reduction 2	0.5615	0.0322	MCMC
α_3	Contact rate reduction 3	0.6051	0.0299	MCMC
μ	Transition rate from E to A/U/I	1/3	–	[5]
ρ_1	Proportionality of transferred E to A	0.3	–	[25]
ρ_2	Proportionality of transferred E to U	0.3	–	[26]
η_1	Recovery rate of A	1/7	–	[10]
η_2	Recovery rate of U	1/7	–	[10]
η_3	Recovery rate of I	1/7	–	[10]
τ	Transition rate from U to I	0.3541	0.0529	MCMC
δ	Disease death rate of I	0.001	9.0254×10^{-5}	MCMC
I_1	Upper limit for contact rate reduction 1	940.29	57.216	MCMC
I_2	Upper limit for contact rate reduction 2	3737.4	209.37	MCMC

Initial Value	Definition	Estimated Mean Value	Standard Deviation	Data Source
$S(0)$	Initial susceptible population	1.457×10^7	–	[7]
$E(0)$	Initial exposed population	6216	583.56	MCMC
$A(0)$	Initial asymptomatic infected population	1940.6	212.93	MCMC
$I(0)$	Initial reported infected population	4344	–	[7]
$U(0)$	Initial unreported infected population	939.35	146.05	MCMC
$R(0)$	Initial recovered population	4194	–	[7]

the average number of infections that an infected individual may cause at time t. The definition of $\mathcal{R}_t$ naturally indicates that a disease may continue to develop and persist in a community if $\mathcal{R}_t > 1$ while the disease declines if $\mathcal{R}_t < 1$. From the parameter values in Table 1, we obtain the estimated values of $\mathcal{R}_t$ in a piecewise format as

$$\mathcal{R}_t = \begin{cases} 1.8371, & \text{if} \quad 0 < I < I_1, \\ 0.9232, & \text{if} \quad I_1 < I < I_2, \\ 0.8327, & \text{if} \quad I_2 < I. \end{cases} \qquad (3.1)$$

The estimated mean values of $I_1 = 940.29, I_2 = 3737.4$, and $I(0) = 4344$ suggest that in a short window of time staring April 16, the contact rate between the susceptible and infected individuals is reduced by $1 - \alpha_3$, which leads to $\mathcal{R}_t = 0.8327$. By referring to the estimated mean value of α_3 in Table 1, we find that the contact rate is effectively reduced by 60% from the contact rate during normal social activities. During this time window, the number of reported infected cases continues to increase
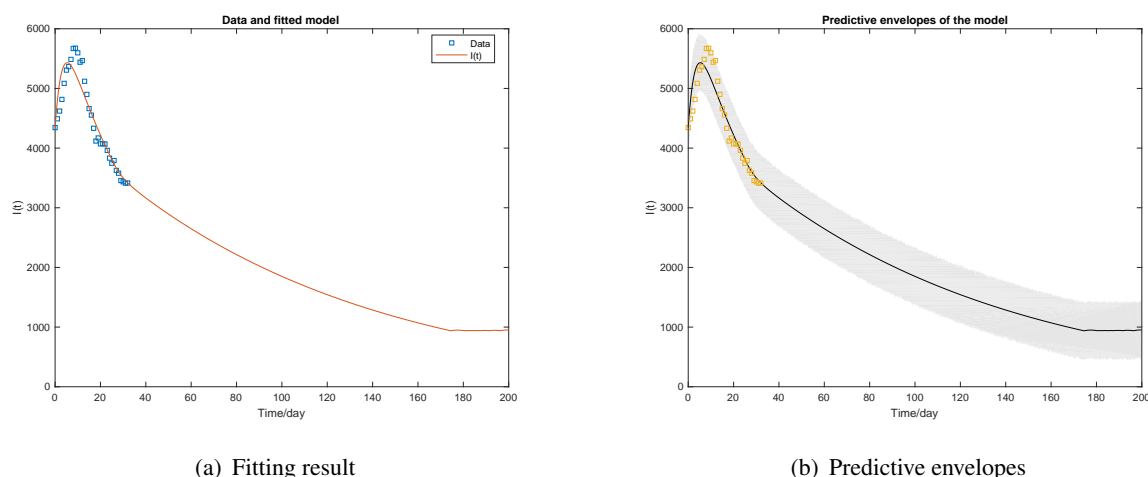
(a) Fitting result   (b) Predictive envelopes

Figure 3. The fitting result of model (2.3) to the reported infected population between April 16 and May 18 in Ontario, Canada. 3(a) shows the fitting of $I(t)$ and the data; 3(b) shows the predictive envelope of $I(t)$. The greyed area in Figure 3(b) demonstrates the 95% CI from the MCMC estimation.

because the population of asymptomatic and unreported infected individuals who are contagious is increasing during this time. However, because $\mathcal{R}_t < 1$, the number of reported infected cases quickly starts to decline. When $I(t)$ reaches I_2, the contact rate between the susceptible and infected population is reduced by a less suppressed degree as $1 - \alpha_2$. Following this new social interaction pattern, the reported infected cases continue to decline but at a slower rate.

Figure 3(a) shows that on May 18, the number of reported symptomatic cases falls between the estimated values of I_1 and I_2. This suggests that following May 18, based on the current public's awareness of practicing physical distancing, the contact rate remains to be reduced by $1 - \alpha_2$. However, with the gradual reopening of businesses provincial wide and less restrictive public heath interventions, community members may lose fear of getting infection at least to some extent. This will inevitably lead to increased social activities and may also result in a bounced back contact rate.

(2) Relaxed physical distancing

To study the impact of relaxed social awareness on the trend of disease spread, we vary values of α_2. Figure 4(a) demonstrates that even with a slightly decreased α_2, the reported symptomatic population bounces back from the originally projected decay. All decreased α_2 predict a second wave of the disease outbreak before the disease status progresses to a plateau phase again. A larger α_2 is also associated with a higher peak of a second wave and an earlier time when the peak attains. Figure 4(a) also indicates that although a second wave is highly like to occur with an increasing contact rate, the magnitude of the second wave is less than the magnitude of the first one.

We also visualize the number of unreported infected cases with different contact rate α_2. Figure 4(b) shows that under the estimated α_2 from Table 1, the unreported infected population is projected to decrease steadily after May 18. By the assumptions of (2.3), the unreported infected individuals are contagious and may transmit the disease. Hence, a declined population in this class will mitigate the further disease outbreak. However, an increased contact rate shifts the trend from decrease to

increase and further leads to an oscillation of the unreported infected cases. The plot of populations in the asymptomatic class A with different α_2 is similar and is thus omitted. Still, individuals in the asymptomatic class are contagious and a number bounced back indicates a halted mitigation of disease spread.
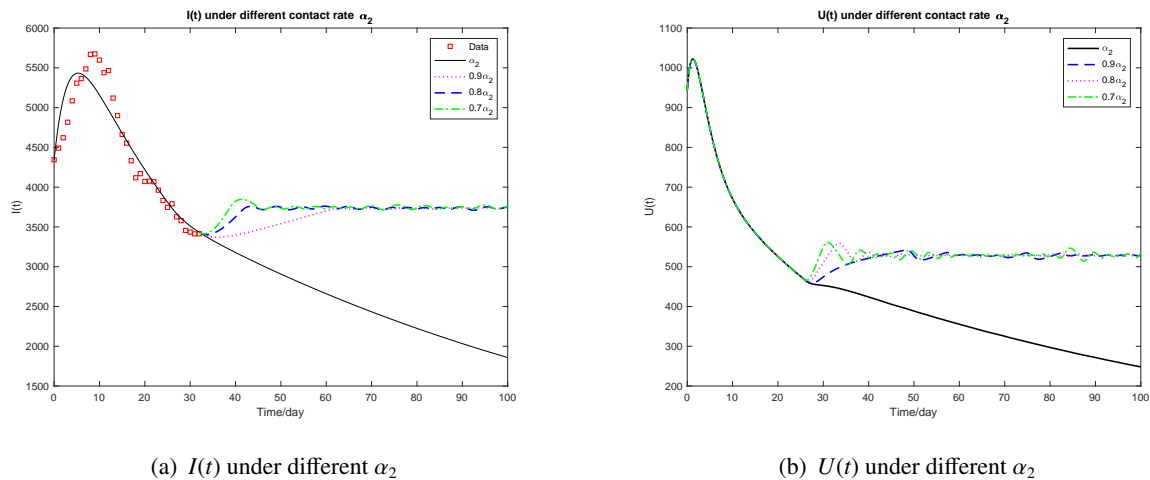

(a) $I(t)$ under different α_2

(b) $U(t)$ under different α_2

Figure 4. Sensitivity analysis with respect to the contact rate α_2. 4(a) shows the number of reported symptomatic individuals under different contact rate α_2; 4(b) shows the number of unreported infected cases with different α_2.
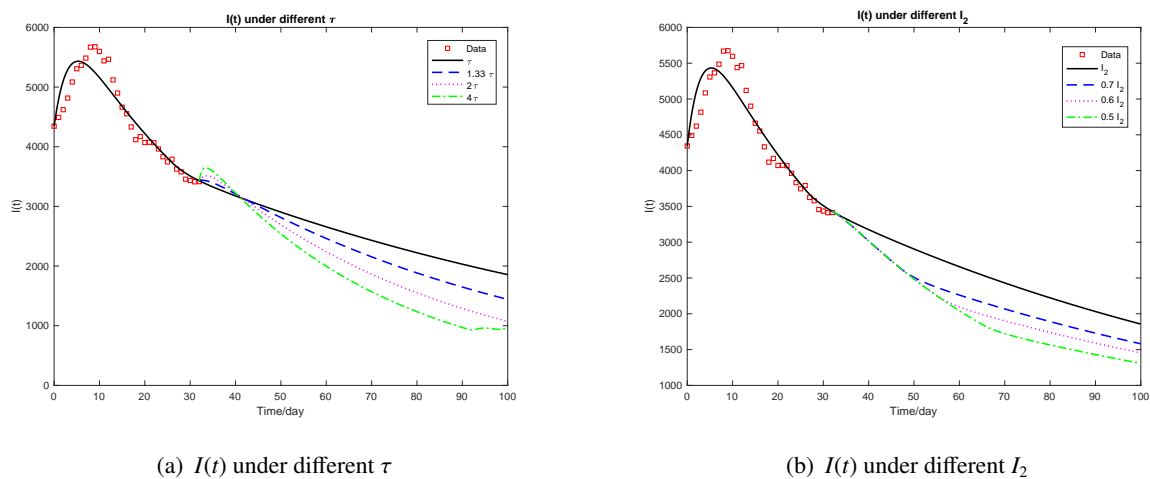

(a) $I(t)$ under different τ

(b) $I(t)$ under different I_2

Figure 5. The reported symptomatic population under different τ and I_2 respectively.

(3) Disease intervention strategy

We explore possible disease intervention strategies that can be manipulated via altering an individual's behavior or affecting an individual's awareness of practicing physical distancing. In model (2.3), parameter $1/\tau$ represents the average waiting time that an infected individual with mild symptoms spends before visiting medical facilities for diagnosis. The unreported infected cases are contagious and may be more active in social interactions than the reported infected cases because they lack con-

firmative information of their infection and therefore are not required to comply with the mandatory self-isolation. Figure 5(a) shows that the number of reported symptomatic cases decreases more rapidly if the average waiting time $1/\tau$ is decreased or equivalently the transition rate from class U to I is increased. Practically, reducing the waiting time by $25\%, 50\%, 75\%$ implies that an individual with mild symptoms now waits for an average of $0.7, 1.4, 2.1$ days less respectively before seeking for medical help. Shortening of the waiting time can be achieved by updating the testing policies. More efficiently and economically, the task can be fulfilled by educating the general public to have the correct altitude towards recognizing the common symptoms of infection and report to public heath agencies in a timely manner.

If the waiting time $1/\tau$ is decreased by $25\%, 50\%, 75\%$ respectively following May 18, the reported infected population increases slightly over a short period of time instead of a monotonic decrease. However, once it is peaked, the reported infected population starts a sharp decrease. Figure 5(a) shows a consistent pattern that the number of reported infected cases stays at a much lower level as long as $1/\tau$ is decreased. This indicates that reducing the waiting time for unreported infected individuals to be diagnosed can effectively mitigate the further disease outbreak.

Figure 5(b) shows the number of reported symptomatic cases under different I_2. With the estimated parameters in Table 1, the fitting projects the decay of reported symptomatic population. A decreased threshold I_2 doesn't change the trend of disease spread. Simulations show a consistent pattern that the reported symptomatic cases decline more quickly with a decreasing number of I_2 following May 18.

Given $I(t) = 3415$ on May 18 and the estimated parameters from Table 1, particularly $I_1 = 940.29, I_2 = 3737.4$, the contact rate remains in the range where it is reduced by $1 - \alpha_2$ for some extended period. However, in simulations, a decreasing I_2 suppresses the contact rate further to $\beta_i(1 - \alpha_3)$ following May 18. Figure 5(b) shows a drastic decline of the reported symptomatic population with a decreased I_2. The result suggests that a greater suppression of contact rates in a wider range leads to a much more controllable epidemic situation.

Note that manipulating the threshold values I_1, I_2 for the piecewise contact rate (2.2) is different from manipulating the contact rate $\beta_i(1 - \alpha_j)$ for $i = 1, 2, j = 1...3$. By varying I_1, I_2, the contact rate within each stage remains unchanged. However, I_1, I_2 are related to the timing of reopening for each stage. From the view of designing disease intervention strategies, the result suggests that it is neither necessary nor practical to impose more restrictive measures to the entire community. The current intervention measures and practice of physical distancing among community members are effective enough to bring down the reported symptomatic cases. However, following the multi-phase reopening plan, the timing when restrictive measures are lifted in each phase is critical. Moreover, it is important to continue educating the public about the importance of practicing physical distancing such that the contact rate remains identical in each phase.

4. Conclusion and discussion

Since the initial identification of COVID-19 in Wuhan, China, the disease quickly rises global public heath concern. In Ontario, Canada, the first positive case was identified in late January, as a case directly linked to travel history. However, evidence of community transmission was later recorded and followed by a serious outbreak starting mid March. The Ontario government then imposed restrictive measures to intervene the disease spread. Because of a lack of effective vaccines, the disease interven-

tion strategies are mainly nonpharmaceutical. Nonessential businesses were closed and people were required to keep a physical distancing when appeared in public. The main objective of these non-pharmaceutical interventions is to reduce the contact rate between susceptible individuals and infected individuals. The restrictive measures combined with the practice of physical distancing are effective in mitigating the disease spread. Starting in May, with a steady decline of the confirmed cases, Ontario government declared a multi-phase reopening plan. The lift of restrictive measures is associated with great concern of a second wave of the disease outbreak.

In this paper, we propose a dynamic model and incorporate a piecewise contact rate between the susceptible and infected population. We consider that the contact rate is not a constant but depends on the severity of disease outbreak. The piecewise contact rate also reflects the public's awareness of practicing physical distancing because individuals are prone to take more precautious measure from contracting the virus if they perceive that the risk of getting infection is high. The risk of infection is linked directly to the total number of infected cases where the data is easily assessable via media reporting.

The model (2.3) is fitted to the data in Ontario, Canada between April 16 and May 18 and the fitting result is good. Based on the estimated parameters, we calculate the effective reproduction number $\mathcal{R}_t$ within each interval. The simulations project that the disease declines steadily but will not disappear in a relatively long time. In a worse scenario, an increasing contact rate α_2 shifts the originally decreasing $I(t)$ to an increasing trend again before $I(t)$ reaches a plateau phase. The result suggests the importance of maintaining the contact rate at a low level in preventing a second wave. Considering the fact that Ontario is entering into a phase of reopening, and normal social activities resume, we investigate strategies that may mitigate the disease outbreak given the contact rates unchanged.

Simulation results show that encouraging individuals with mild symptoms to visit medical facilities and get diagnosis as soon as possible is an effective disease intervention strategy. The results also show that given the identical effectiveness of practicing physical distancing, imposing more restrictive measures for some extended period even when disease is less severe facilitates the disease decline.

Our model can be further calibrated to include multi-groups such as individuals in different ages, geographical locations etc. In order to do that, the data needs a further investigation accordingly, which leaves as further work.

Acknowledgement

Conflict of interest

The author declares there is no conflict of interests.

References

1. World Health Organization, (2020). Available from: `https://www.who.int/emergencies/diseases/novel-coronavirus-2019`.

2. N. van Doremalen, T. Bushmaker, D. H. Morris, M. G. Holbrook, A. Gamble, B. N. Williamson, et al., Aerosol and surface stability of SARS-CoV-2 as compared with SARS-CoV-1, *N. Engl. J. Med.*, **382** (2020), 1564–1567.

3. X. He, E. H. Y. Lau, P. Wu, X. Deng, J. Wang, X. Hao, et al., Temporal dynamics in viral shedding and transmissibility of COVID-19, *Nat. Med.*, **26** (2020), 672–675.

4. A. J. Kucharski, T. W. Russell, C. Diamond, Y. Liu, J. Edmunds, S. Funk, et al., Early dynamics of transmission and control of COVID-19: a mathematical modelling study, *Lancet Infect. Dis.*, **20** (2020), 553–558.

5. Q. Li, X. Guan, P. Wu, X. Wang, L. Zhou, Y. Tong, et al., Early transmission dynamics in Wuhan, China, of novel coronavirus-infected pneumonia, *N. Engl. J. Med.*, **382** (2020), 1199–1207.

6. The novel coronavirus pneumonia emergency response epidemiology team, The epidemiological characteristics of an outbreak of 2019 novel coronavirus disease (COVID-19)–China, *China CDC Weekly*, **2** (2020), 113–122.

7. *Epidemiologic Summary: COVID-19 in Ontario: January 15, 2020 to May 18, 2020*, Ontario Goverment, (2020). Available from: `https://files.ontario.ca/moh-covid-19-report-en-2020-05-18.pdf`.

8. S. He, S. Tang, L. Rong, A discrete stochastic model of the COVID-19 outbreak: Forecast and control, *Math. Biosci. Eng.*, **17** (2020), 2792–2804.

9. K. Iwata, C. Miyakoshi, A simulation on potential secondary spread of novel coronavirus in an exported country using a stochastic epidemic SEIR model, *J. Clin. Med.*, **9** (2020), 944.

10. Z. Liu, P. Magal, O. Seydi, G. Webb, Understanding unreported cases in the COVID-19 epidemic outbreak in Wuhan, China, and the importance of major public health interventions, *Biology*, **9** (2020), 50.

11. Z. Liu, P. Magal, O. Seydi, G. Webb, A COVID-19 epidemic model with latency period, *Infect. Disease Model.*, **5** (2020), 323–337.

12. S. Ruan, Likelihood of survival of coronavirus disease 2019, *Lancet Infect. Dis.*, **20** (2020), 630–631.

13. B. Tang, X. Wang, Q. Li, N. L. Bragazzi, S. Tang, Y. Xiao, et al., Estimation of the transmission risk of the 2019-nCoV and its implication for public health interventions, *J. Clin. Med.*, **9** (2020), 462.

14. C. Yang, J. Wang, A mathematical model for the novel coronavirus epidemic in Wuhan, China, *Math. Biosci. Eng.*, **17** (2020), 2708–2724.

15. W. Zhou, A. Wang, F. Xia, Y. Xiao, S. Tang, Effects of media reporting on mitigating spread of COVID-19 in the early phase of the outbreak, *Math. Biosci. Eng.*, **17** (2020), 2693–2707.

16. H. Zhao, Z. Feng, Staggered release policies for COVID-19 control: Costs and benefits of relaxing restrictions by age and risk, *Math. Biosci.*, **326** (2020), 108405.

17. E. Abdollahi, M. Haworth-Brockman, Y. Keynan, J. M. Langley, S. M. Moghadas, Simulating the effect of school closure during COVID-19 outbreaks in Ontario, Canada, *BMC Med.*, **18** (2020), 1–8.

18. B. Tang, F. Scarabel, N. L. Bragazzi, Z. McCarthy, M. Glazer, Y. Xiao, et al., De-escalation by reversing the escalation with a stronger synergistic package of contact tracing, quarantine, isolation and personal protection: feasibility of preventing a COVID-19 rebound in Ontario, Canada, as a Case Study, *Biology*, **9** (2020), 100.

19. A. R. Tuite, D. N. Fisman, A. L. Greer, Mathematical modelling of COVID-19 transmission and mitigation strategies in the population of Ontario, Canada, *CMAJ*, **192** (2020), E497–E505.

20. J. Wu, B. Tang, N. L. Bragazzi, K. Nah, Z. McCarthy, Quantifying the role of social distancing, personal protection and case detection in mitigating COVID-19 outbreak in Ontario, Canada, *J. Math. Ind.*, **10** (2020), 15.

21. O. Diekmann, J. A. P. Heesterbeek, *Mathematical Epidemiology of Infectious Diseases: Model Building, Analysis and Interpretation*, John Wiley, (2000).

22. H. Nishiura, G. Chowell, The effective reproduction number as a prelude to statistical estimation of time-dependent epidemic trends, in *Mathematical and Statistical Estimation Approaches in Epidemiology*, Springer, Dordrecht, (2009).

23. P. Van den Driessche, J. Watmough, Reproduction numbers and sub-threshold endemic equilibria for compartmental models of disease transmission, *Math. Biosci.*, **180** (2002), 29–48.

24. K. Mizumoto, K. Kagaya, A. Zarebski, G. Chowell, Estimating the asymptotic proportion of coronavirus disease 2019 (COVID-19) cases on board the Diamond Princess cruise ship, Yokohama, Japan, 2020, *Euro Surveill.*, **25** (2020), 12.

25. H. Nishiura, T. Kobayashi, T. Miyama, A. Suzuki, S. Jung, K. Hayashi, et al., Estimation of the asymptomatic ratio of novel coronavirus infections (COVID-19), *Int. J. Infect. Dis.*, **94** (2020), 154–155.

26. C. Wang, L. Liu, X. Hao, H. Guo, Q. Wang, J. Huang, et al., Evolving epidemiology and impact of non-pharmaceutical interventions on the outbreak of coronavirus disease 2019 in Wuhan, China, *MedRxiv*, https://doi.org/10.1101/2020.03.03.20030593.

27. *Interim Clinical Guidance for Management of Patients with Confirmed Coronavirus Disease (COVID-19)*, CDC, (2020). Available from: https://www.cdc.gov/coronavirus/2019-ncov/hcp/clinical-guidance-management-patients.html.

28. H. Haario, M. Laine, A. Mira, E. Saksman, DRAM: Efficient adaptive MCMC, *Stat. Comput.*, **16** (2006), 339–354.